The self-assembly of copolymers with one hydrophobic and one polyelectrolyte block in aqueous media. Dissipative particle dynamics study

Martin Lísal[1,2], Zuzana Limpouchová[3] and Karel Procházka[3*]

[1]*Laboratory of Aerosols Chemistry and Physics, Institute of Chemical Process Fundamentals of the CAS, v. v. i., Rozvojová 135/1, 165 02 Prague 6-Suchdol, Czech Republic*

[2]*Department of Physics, Faculty of Science, J. E. Purkinje University, České Mládeže 8, 400 96 Ústí n. Lab., Czech Republic*

[3]*Department of Physical and Macromolecular Chemistry, Faculty of Science, Charles University in Prague, Hlavova 2030, 128 40 Prague 2, Czech Republic*

[*]to whom correspondence should be sent

SUPPORTING INFORMATION

Model and Method

Dissipative Particle Dynamics (DPD)

In the last decade, the coarse-grained dissipative particle dynamics (DPD) simulations have proven a suitable tool for studying polymer systems. Since Groot and Warren established a link between the Flory-Huggins and soft-repulsion parameters used in DPD,[1] a number of neutral polymer systems have been successfully studied.[2-5] Later electrostatics were implemented into the model[6-9] and polyelectrolyte (PE) systems were addressed.[10, 11] At present, studies of complex PE systems based on alternative models that do not treat electrostatics explicitly have also been published.[12-16] However, we are of the opinion that the explicit treatment of electrostatic forces should be an intrinsic part of simulations of PEs, because it corresponds to real physics and allows reasonably good emulation of the contribution of counterions to the entropy of the system, which the other approaches do not secure.

In simulations, a DPD particle represents a fluid element which contains a number of solvent molecules, solvated ions or several polymer segments. We thus treated the solvent (S),

counterions (CI) and co-ions (I^+ and I^-) as different types of DPD particles. The DPD ions can be regarded as ions solvated by several layers of solvent. We represent the diblock copolymer by two flexible (linearly connected) chains of DPD particles with lengths $n = 5$ and $m = 5$, connected end-to-end and composed of A- and B-types of DPD particles. We modeled the DPD particles as being purely repulsive and the ij -pairs of particles interacting via a soft repulsive potential[1, 4]

$$\begin{aligned} u_{ij}^{\mathrm{sr}} &= \frac{a_{ij}}{2} r_{\mathrm{c}} \left(1 - \frac{r_{ij}}{r_{\mathrm{c}}}\right)^2 \qquad \left(r_{ij} < r_{\mathrm{c}}\right) \\ &= 0 \qquad\qquad\qquad\qquad \left(r_{ij} \geq r_{\mathrm{c}}\right) \end{aligned} \tag{1}$$

where a_{ij} is the maximum repulsion between particles i and j, r_{ij} is the separation distance, and r_{c} is the cut-off radius.

Diblock copolymers $A_5B(+)_5$ consist of DPD particles connected in a chain using harmonic spring potentials:

$$u_{i,i+1}^{\mathrm{hs}} = \frac{K}{2}\left(r_{i,i+1} - r_0\right)^2 \tag{2}$$

which act between adjacent particles i and $i+1$ in addition to the soft repulsive interaction. In Eq. (2), K is the spring constant and r_0 is the equilibrium distance. A value of $K/(kT)$ between 2 and 4 (k is the Boltzmann constant and T is the temperature) and $r_0 = 0$ are typically utilized.[1]

In the system of interest, the shell-forming B^+-segments of $A_5B(+)_5$ chains, the counterions and the co-ions are charged. Since the DPD particles are modeled as soft particles, the charge is spread over a finite volume using the Slater smearing charge distribution[8]

$$f(r) = \frac{qe}{\pi\lambda^3} \exp\left(-\frac{2r}{\lambda}\right) \tag{3}$$

The charge smearing prevents the collapse of beads on top of each other in the case of unlike point charges.[6-9] In Eq. (3), q is the relative charge, e is the electron charge and λ is the decay length of the charge. The electrostatic interaction between charged particles i and j is then defined by

$$u_{ij}^{\mathrm{el}} = \frac{q_i q_j}{r_{ij}} \lambda_{\mathrm{B}} kT\left[1 - \left(1 + \beta r_{ij}\right)\exp\left(-2\beta r_{ij}\right)\right] \tag{4}$$

where $\lambda_B = e^2/(4\pi\varepsilon_0\varepsilon_r kT)$ is the Bjerrum length (ε_0 is the dielectric constant of a vacuum and ε_r is the relative permittivity of the reference medium), q_i and q_j are their partial charges and $\beta = 5/(8\lambda)$.

Groot and Warren [1] mapped the DPD model onto the Flory-Huggins (FH) model and established a link between a_{ij} and the chi-parameter χ_{ij}:

$$\chi_{ij} = 2C\rho r_c^3 \left(a_{ij} - \frac{a_{ii} + a_{jj}}{2} \right) \frac{r_c}{kT} \tag{5}$$

where ρ is the total particle density and C is a constant depending on ρ. Assuming $a_{ii} = a_{jj}$ and using the equation of state for the soft repulsive DPD fluid together with the compressibility value for ambient water, Groot and Warren derived an expression for like-repulsive parameters:

$$\frac{a_{ii} r_c}{kT} \equiv \frac{a_{jj} r_c}{kT} = \frac{75}{\rho r_c^3} \tag{6a}$$

They further obtained linear relationships between a_{ij} and χ_{ij} for $\rho r_c^3 = 3$:

$$\frac{a_{ij} r_c}{kT} = \frac{a_{ii} r_c}{kT} + 3.27\chi_{ij} \tag{6b}$$

We controlled the solvent quality for A and B blocks of $A_5B(+)_5$ by parameters a_{AS} and a_{BS}, respectively, and the incompatibility between A and B blocks by parameter a_{AB}. Other details regarding the DPD method were given in the Supporting Information of our previous paper.[10]

Simulation Details

We mimic aqueous copolymer solutions using $A_5B(+)_5$ immersed in a mixture of solvent particles, counter- and co-ions. The volume fraction of $A_5B(+)_5$ in the system is $F_t = 0.0512$. For comparison, we also performed simulations for neutral diblock copolymers. In the DPD method, the following reduced units were used: r_c is the unit of length, the unit of mass is the mass of a DPD particle and the unit of energy is kT; these terms are used throughout this work. All the DPD simulations were carried out at a total particle density of $\rho = 3$ in a cubic box of 25x25x25 with noise amplitude $\sigma_{ij} = 3$ and time step $\Delta t = 0.05$.

Using the reduced units, we set the repulsion parameter between like particles at $a_{ii} \equiv a_{jj} = 25$. In this study, we performed a series of simulations for systems formed by very hydrophobic A block (a_{AS} = 40) and an annealed PE B block. First, we assumed that the B-block (even in the non-charged neutral state) is soluble ($a_{BS} = 25$), and the incompatibility between the A and B blocks varies in the range, a_{AB} = 25 – 40. The above parameters correspond to the bead-bead chi-interaction parameters $\chi_{AS} = 0 - 4.6$, $\chi_{AB} = 0 - 4.6$ and $\chi_{SB} = 0$, respectively. In the next runs, we deteriorated the solvent quality for the polyelectrolyte block (a_{BS} = 25 – 40) to mimic the fact that the backbone of a number of real PEs is in fact hydrophobic. For the harmonic spring potential, we used the spring constant $K = 4$ and equilibrium distance $r_0 = 0$. We further assumed that the values of a_{ij} for the counter- and co-ions are the same as those for the solvent particles. In addition, we looked at two systems where the values of a_{ij} for the ions were set to 25.

We further used the decay length of the charge $\lambda = 0.2$ and Bjerrum length $\lambda_B \cong 1.10$, which correspond to the aqueous environment.[6, 7] The long-range electrostatic interactions were treated using the Ewald sum with cut-off $r_c^{el} = 3$, real-space convergence parameter $\alpha^{ES} = 0.975$ and reciprocal vector range $\boldsymbol{n}_{max} = (5,5,5)$.[8] The size of the simulation box is 25^3 and the periodic boundary conditions are applied in all three directions.

Simulations typically started from random configurations but, in a few cases, simulations were also initiated from the associated state. After an equilibration period of $2 \cdot 10^6$ time steps, we typically ran $(20 - 50) \cdot 10^6$ time steps for aggregated systems and $5 \cdot 10^6$ time steps otherwise. DPD trajectories were generated using the GNU program DL_MESO,[17] followed by post-processing to evaluate the quantities of interest.

We studied the effect of the charge smearing very carefully and published the most important results in our earlier papers. In reference 59, we actually calibrated the parameters of forces by mapping the simulation results onto experimental data. The value λ = 0.2 is the largest value for which the whole charge is localized inside the coarse-grained bead. We have shown that the condensation of charges on top of each other for a_{ij} = 25 does not occur. Here we add the comparison of the most important features for λ = 0.2 and also for the value λ = 0.67 used by some other authors (K. Šindelka: MSc Thesis. Charles University, Prague, 2014).

Distribution of exponentially smeared charge

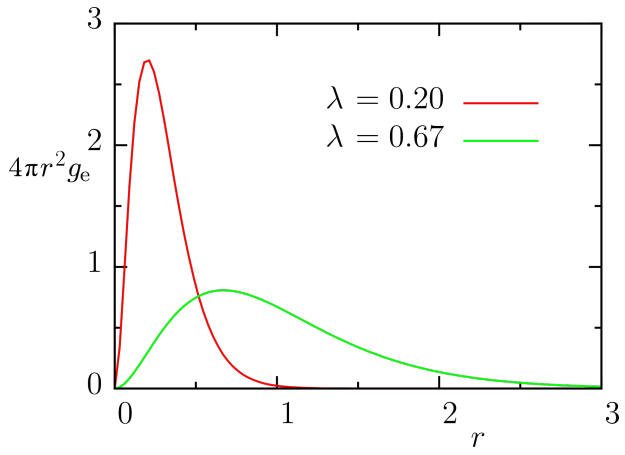

Fig. 1. Spatial density $g(r)$ of the exponentially smeared charge for different values of the decay constant λ.

Fig. 1 depicts the distribution of the exponentially smeared charge. It shows that for $\lambda = 0.67$, the charge is delocalized in a very broad region.

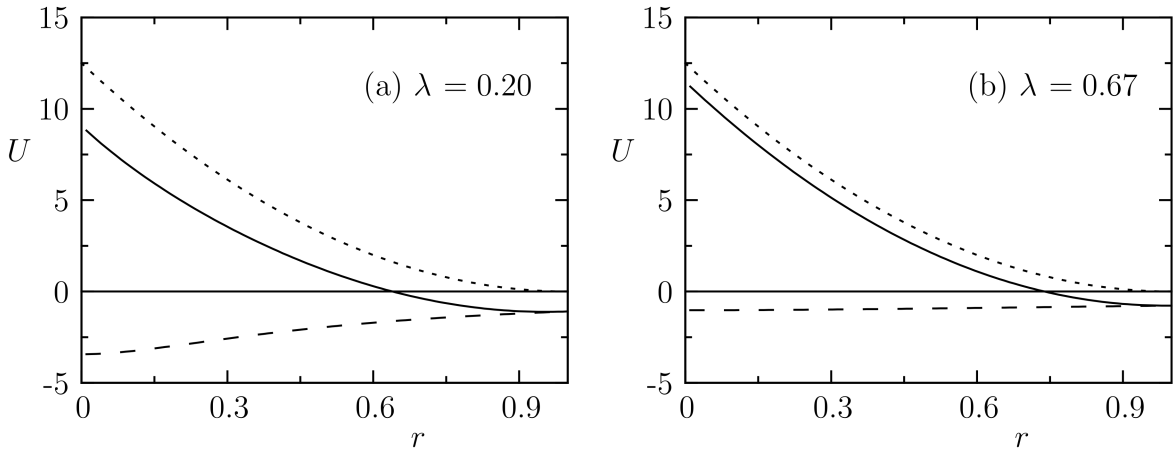

Fig. 2. Sum of the DPD repulsive potential with a_{ij} = 25 and the smeared electrostatic potential of two oppositely charged clouds (with charges +e and -e) for $\lambda = 0.2$ and $\lambda = 0.67$. Full lines represent the sum of electrostatic and repulsive potential, which are drawn in dashed and dotted lines, respectively.

Fig. 2 shows the effect of charge smearing on pair interactions. It compares the electrostatic potential between two oppositely charged beads (dotted curve – long ticks) with the soft DPD potential for favorably interacting beads with a_{ij} = 25 (dotted curve – short ticks). Solid line depicts their combination. The charges of beads are: +e and –e. The comparison shows that the resulting soft force is just little less repulsive than that for neutral beads.

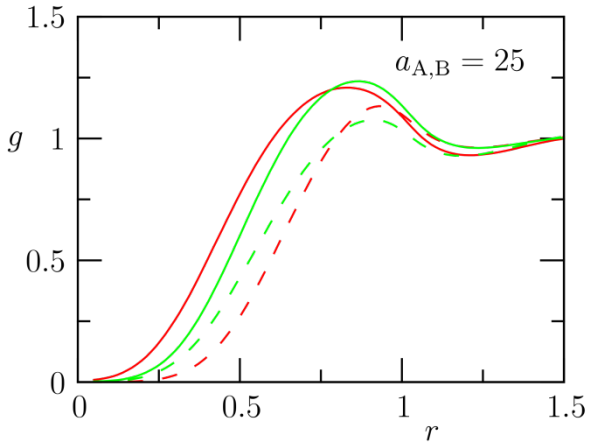

Fig. 3. Radial distribution function, g, for the mixture of opositely charged beads. Red lines correspond to λ = 0.2, while the green lines represent and λ = 0.67. Full lines are radial distribution functions between unlike particles, $g_{A\text{-}B}$, and the dashed ones are radial distribution functions between like particles, $g_{A\text{-}A}$ and $g_{B\text{-}B}$.

Fig. 3 compares the radial distribution function in the system containing charged monomer beads. Red curves are for λ = 0.20 and green for λ = 0.67. Full curves show g_{+-} between oppositely charged beads and dotted curves depict g_{++} between beads with charges of the same sign.

The curves clearly prove that the use of the decay constant λ = 0.20 secures that (i) whole charge is localized within one bead and local correlation effects are taken into consideration at the coarse-grained level, (ii) opposite charges do not collapse on the top of each other, and (iii) the resulting force between beads is soft and it is not necessary to shorten the integration step in simulations of charged systems.

Evaluation of Characteristics Measured by Light Scattering

The intensity of scattered light is proportional to the second power of the volume of the scattering object (i.e., to the sixth power of its effective radius) and therefore static light scattering (SLS) measurement yields the z-average radius of gyration, $\langle R_G \rangle_z$ and dynamic light

scattering (DLS) measurement yields the z-average translational diffusion coefficient, $\langle D_{tr}\rangle_z$ which is inversely proportional to the hydrodynamic radius, $\langle R_H\rangle_z$. Both methods are very sensitive to the presence of large species in disperse polymer samples. This means that, in massively associating polymer systems, both SLS and DLS almost completely disregard unimer and yield data that roughly correspond to associates. In simulations we can evaluate all the weighted averages of the gyration radius of associates, i.e., the number average $\langle R_G\rangle_n$, weight-average $\langle R_G\rangle_w$, as well as the *z*-average $\langle R_G\rangle_z$. Fig. 2 in the main text shows a plot of $\langle R_G\rangle_z$ vs. α (curve 1). The dependence decreases in the whole $\alpha \in \langle 0, 1)$ region reflecting the decrease in $\langle A_s\rangle_w$. The decrease is rapid in the region of $\alpha \in \langle 0, 0.5)$, and then slows down and the curve almost levels off for α approaching 1.

The evaluation of $\langle D_{tr}\rangle_z$ for scattering objects is a formidable task because the associates are dynamic species and their association number continuously changes with time. Therefore, instead of $\langle D_{tr}\rangle_z$, we evaluated the number average diffusion coefficient D_{com} for all the chains (regardless of whether they are free or engaged in associates). The evaluation is simple, but the precise physical meaning of D_{com} requires an explanation. In a non-associated system, D_{com} describes the diffusion of single chains. In self-assembled systems, it reflects the complex motion of both free (non-associated) chains and chains entrapped in associates. In systems containing a large excess of high-molar-mass associates, most chains are involved in associates and their motion corresponds to that of the associates. In this case, the DPD simulation yields roughly the number average $D_{com} \cong \langle D_{tr}\rangle_n$ of associates, which is (due to the applied weighting procedure) appreciably larger than corresponding $\langle D_{tr}\rangle_z$ measured by DLS. However, as both dependences, i.e., D_{com}, as well as $\langle D_{tr}\rangle_z$ vs. α, reflect the same changes in $F_w(A_s)$ vs. α, their basic shapes are similar. Knowledge of the diffusion coefficient allows us to evaluate the radius of an equivalent hydrodynamic sphere, called the hydrodynamic radius, R_H, on the basis of the Stokes-Einstein equation,[18] which postulates that both characteristics are inversely proportional to each other. Curve 2 shows the dependence of $(D_{com})^{-1}$ on α, which decreases similarly to the $\langle R_G\rangle_z$ values.

Salt Effect on Associates with Hydrophobic PE Blocks

The addition of salt induces similar changes as those in systems with readily soluble Bsegments, i.e., electrostatic screening promotes the formation of large associates. However the effect is more pronounced (aggregates in salty solutions are formed by larger numbers of chains) and it assists the “closed association” mechanism. For illustration in Fig. 4, we depict

the salt-induced changes in $F_w(A_s)$ for systems with α=0.75. The shift in the peak of associates to higher A_s accompanied by its separation from the unimer peak with increasing salt content, are very pronounced. The addition of the salt actually changes the character of the association from an "open" to a "closed" one.

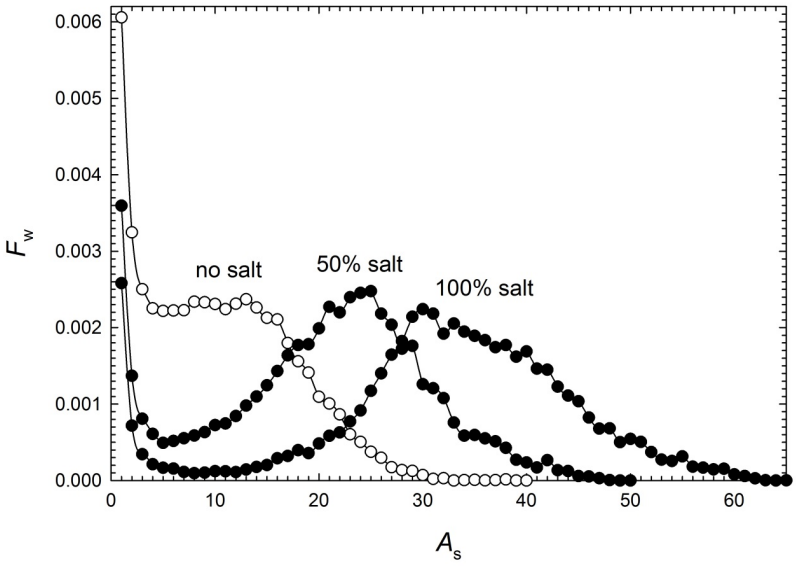

Fig. 4. Effect of salt on the weight distribution functions, $F_w(A_s)$, of association numbers A_s for a system with a_{AS}=$a_{A\text{-}CI}$=40, a_{BS} =32.5, $a_{B\text{-}CI}$=25 and a_{AB}=40, and with α=0.75.

The Conversion of α Scale into pH Scale (Explanatory Comments)

The approximate recalculation of characteristics of associates depending on the degree of ionization α into dependencies on pH can be substantiated as follows. Since we use α as an increasing input parameter and assume that it is equal to the neutralization degree, our computer study emulates the titration of polyacid by an alkaline hydroxide. The protons are replaced by alkali metal ions from the added base and they recombine with OH^- obeying the auto-dissociation equilibrium described by K_w ca. 10^{-14}. The polyacid is continuously converted into polysalt and the mixture of the weak acid and its salt behaves like a dilute buffer. In the most interesting pH region from 4 to 10, the concentrations of H_3O^+ and OH^- do not exceed 10^{-4} mol/L, but the concentrations of ionized and protonized structural units of polymer chains depend on α and on the overall concentration of PE block, and exceed the maximum concentrations of H_3O^+ and OH^- by ca. two orders of magnitude. Note that the concentration of ionized units and counterions equals to the concentration of virtually added

base. Therefore, our model does not take H_3O^+ and OH^- ions a priori into account, we include only the alkaline ions into the simulation scheme (similarly to other authors) and for the evaluation of pH, we use a simple textbook Eq. (1) in the main text.

In the main text, we explained that the conversion of α into the pH scale is only approximate, but the recalculation of pH values requires a short additional explanation. Simple Eq. (1) applies to a homogeneous solution and yields spatially constant bulk pH, but the studied system is spatially inhomogeneous at short length scales. At low α, the ionization is localized in the region of micellar shells and therefore the majority of the counterions also concentrate in shells and in their immediate vicinity. At high α, the charges are distributed more homogeneously throughout the system compared with strongly associating systems, but the ionization is still localized on individual polymer chains and on small associates. Experimental studies indicate that local ionization degree α_{loc} is suppressed in micellar shells formed by annealed PEs because the concentration of chargeable groups is high and this is why, e.g., the pH-promoted expansion of micellar shells in kinetically frozen (i.e., non-reorganizing) polystyrene-*b*-poly(methacrylic acid) micellar systems is observed by experimentalists at higher bulk pH values (which are currently measured by experimentalists) than pK_A.[19, 20] Recently, it was demonstrated by fluorescence measurements on PE chains tagged by fluorescent pH-indicators that not only the local pH in the micellar shells, but also the local pH close to the PE chain differs from that in bulk and that it even depends on the position of the fluorescent tag along the contour length of the chain. [21] Because the ionization occurs in studied systems at copolymer chains, the charges in the associating systems are mostly localized in micellar shells and the recalculation based on Eq. (1) yields the effective pH, which is close to the local pH of the shell. It is necessary to keep in mind that this value differs from the value that would be measured by experimentalists, who would observe massive changes in $\langle A_s \rangle_w$ at higher bulk pHs (ca. by one pH unit).

The impact of the length of copolymer blocks on the ionization degree-dependent self-assembly

This paragraph was added as a response to the reviewer suggestion to perform simulations for longer chains in order to demonstrate that the observed behavior is general, i.e., that a similar decrease in A_s with increasing α occurs in systems differing in the length of simulated chains.

The A_5B_5 copolymer chains used in a majority of performed simulations are relatively short and a danger, that gradual decrease of the association number with increasing ionization due to massive dissociation and reorganization of micelles is significantly facilitated in systems with short copolymer blocks, and a possibility, that the associates formed by longer chains could behave differently, cannot be a priori ruled out. Therefore, we performed a series of simulations for longer copolymer chains A_8B_8. The aim of these supplementary simulations is to prove that the observed dissociation of micelles with increasing ionization of their shell-forming blocks is a general phenomenon and applies also for long chains (as it was predicted by scaling theories for polymer chains of realistic length.[22] The simulations with explicit electrostatics are time-consuming and A_8B_8 chains represent the limit of our computational capabilities (one simulation takes ca. two weeks on a supercomputer).

Before we present the supplementary simulation data, we would like to underline that DPD is a coarse-grained method and interaction parameters describing the interaction of coarse-grained polymer beads with coarse-grained solvent beads have been recalculated from the FH parameter, χ, which describes the interaction of one FH segment, which roughly corresponds to one Kuhn segment, i.e., ca. to 5 monomer units (depending on chain flexibility). This means that the coarse-grained A_5B_5 chain emulates a copolymer containing ca. 50 monomer units and the coarse-grained A_8B_8 chain emulates that formed by ca. 80 monomer units.

The methodology of simulations for systems with different block length at constant solvent quality (selectivity) requires a short explanation. As already mentioned, interaction parameters characterizing solvent quality (interaction of polymer beads with the solvent) have been recalculated from the FH parameters, χ. In the limit of infinitely long chains, the value $\chi = 0$ corresponds to a good (athermal) solvent, $\chi = ½$ describes θ-solvent and solvents with $\chi > ½$ are poor solvents (or non-solvents). However, the miscibility of polymers with poor solvents (i.e., solubility) and miscibility of different polymers depend on chain length. The miscibility of chemically different homopolymers deteriorates (decreases) with the polymerization degree N. The condition for phase separation in mixtures of two different chains A_N and B_N of the same length N can be expressed as: $N\chi_{AB} = 10$, where χ_{AB} describes mutual interaction of beads A and B. The above formula can be regarded as a definition of the "critical interaction parameter" (the lowest parameter) which prevents miscibility or dissolution of chains in the solvent. It shows how the "apparent solvent quality" (defined by χ) for chains of different length depends on the chain length. It follows that fairly high χ-

parameters are used in simulations. To get reasonable comparison, the above condition has to be taken into account and the interaction parameter of the hydrophobic bead with the solvent, χ_{AS} has to be appropriately recalculated from $N = 5$ ($\chi_{AS} = 4.6$ and $a_{AS} = 40$) to $N = 8$. A simple recalculation (derived from the phase separation condition, i.e., $N_1(\chi_{AS})_1 = N_2(\chi_{AS})_2$) yields $\chi_{AS} = 2.88$ and $a_{AS} = 34.4$. Because we perform supplementary simulations for systems with hydrophilic PE block B only, the interaction of beads B with solvent is favorable and $\chi_{BS} = 0$ ($a_{BS} = 25$) in both cases. The criterion for the "quality of recalculation" of interaction parameters should be based on the comparison of A_s of non-charged amphiphilic micelles formed by A_5B_5 and A_8B_8 chains. Comment: The association numbers should obey the theoretically predicted scaling rules and if we use the classical formula proposed by Nagarajan and Ganesh,[23] $A_s \propto N_A^{1.19} N_B^{-0.51}$, we should obtain: $A_s(8)/A_s(5) = 1.4$, but we do not expect that the system described by interaction parameters obtained via simple recalculation would accurately obey the scaling laws.

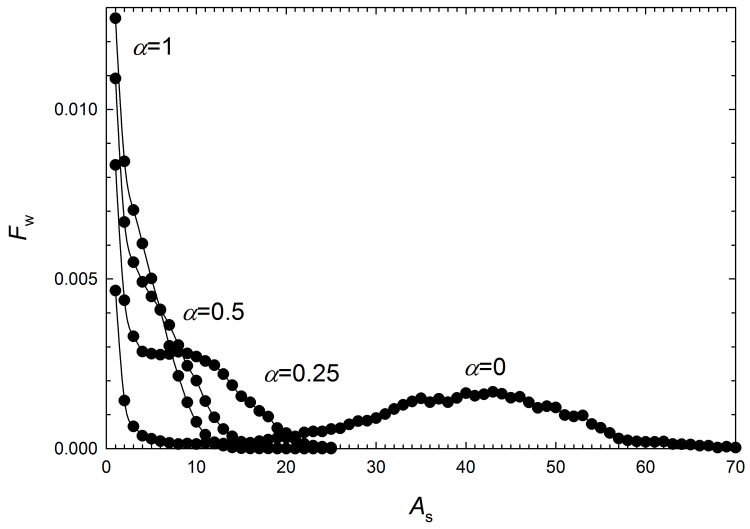

Fig. 5. Distributions of A_s of associates formed by A_8B_8 chains in a solvent which is poor for A beads (simple recalculation of a_{AS}, i.e., $a_{AS} = 34.4$) and good for B beads ($a_{BS} = 25$).

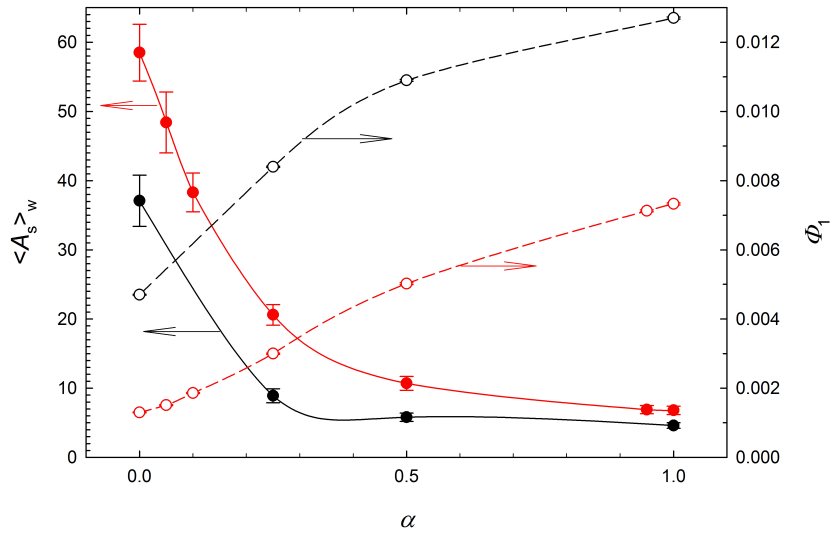

Fig. 6. Comparison of $\langle A_s \rangle_w$ versus α dependences (full curves) and the fraction of non-associated chains, ϕ_1 versus α (dashed curves) for self-assembling systems of A_5B_5 (red color) and A_8B_8 (black color) chains.

Even though the approximate recalculation does not provide optimum values of interaction parameters, we believe that we get reasonable results for persuasive qualitative proof that the behavior observed in simulations is not the artifact. To get more insight into the problem, we performed two series of simulations for a_{AS} = 40 and 34.4. In the first case (a_{AS} = 40) we found that the electrically neutral polymer A_8B_8 does not dissolve in aqueous medium due to too high effective hydrophobicity of A block (the chains macroscopically phase separate). The chains with fully ionized blocks B dissolve in water and are present as unimers and low associates. The associates are present in non-negligible fractions. The average A_s of associates is ca. 12, i.e., slightly higher than that for A_5B_5 (ca. 10).

The results of simulations for a_{AS} = 34.4 are depicted in Fig. 5 and the comparison of A_5B_5 and A_8B_8 systems is shown in Fig. 6. It is obvious that the simple recalculation formula did not secure optimum self-consistency of interaction parameters for different chain lengths. The distributions of A_s for A_8B_8 chains are shifted to lower A_s (Fig. 5). This means that the interaction parameter a_{AS} = 34.4 corresponds to a slightly better solvent for A beads in A_8B_8 system than a_{AS} = 40 in A_5B_5 system. The average association number of the neutral associate and A_s of all other associates formed by A_8B_8 at increasing degrees of association are lower than corresponding A_s of associates formed by A_5B_5 chains (Fig. 6).

Nevertheless, the supplementary simulations for longer chains clearly show that A_s of longer chains decreases similarly to that of shorter chains. This, we believe, provides a sufficient proof that the simulation results are not invalidated by relatively short chains and that the observed behavior is in line with conclusions drawn from mean-field theories.[22]

References

1. R. D. Groot and P. B. Warren, *Journal of Chemical Physics*, 1997, **107**, 4423-4435.
2. E. Moeendarbary, T. Y. Ng and M. Zangeneh, *International Journal of Applied Mechanics*, 2010, **2**, 161-190.
3. X. R. Cao, G. Y. Xu, Y. M. Li and Z. Q. Zhang, *Journal of Physical Chemistry A*, 2005, **109**, 10418-10423.
4. Z. Li and E. E. Dormidontova, *Macromolecules*, 2010, **43**, 3521-3531.
5. R. Bautista-Reyes, C. Soto-Figueroa and L. Vicente, *Molecular Simulation*, 2015, **41**, 663-673.
6. R. D. Groot, *Journal of Chemical Physics*, 2003, **118**, 11265-11277.
7. R. D. Groot, *Journal of Chemical Physics*, 2003, **119**, 10454-10454.
8. M. Gonzalez-Melchor, E. Mayoral, M. E. Velazquez and J. Alejandre, *Journal of Chemical Physics*, 2006, **125**.
9. C. Ibergay, P. Malfreyt and D. J. Tildesley, *Journal of Chemical Theory and Computation*, 2009, **5**, 3245-3259.
10. Z. Posel, Z. Limpouchová, K. Šindelka, M. Lísal and K. Procházka, *Macromolecules*, 2014, **47**, 2503-2514.
11. K. Šindelka, Z. Limpouchová, M. Lísal and K. Procházka, *Macromolecules*, 2014, **47**, 6121-6134.
12. Z. L. Luo and J. W. Jiang, *Journal of Controlled Release*, 2012, **162**, 185-193.
13. S. Y. Nie, Y. Sun, W. J. Lin, W. S. Wu, X. D. Guo, Y. Qian and L. J. Zhang, *Journal of Physical Chemistry B*, 2013, **117**, 13688-13697.
14. M. R. Rodriguez-Hidalgo, C. Soto-Figueroa and L. Vicente, *Soft Matter*, 2013, **9**, 5762-5770.
15. M. R. Rodriguez-Hidalgo, C. Soto-Figueroa and L. Vicente, *Soft Matter*, 2011, **7**, 8224-8230.
16. N. K. Li, W. H. Fuss, L. Tang, R. Gu, A. Chilkoti, S. Zauscher and Y. G. Yingling, *Soft Matter*, 2015, **11**, 8236-8245.

17. M. A. Seaton, R. L. Anderson, S. Metz and W. Smith, *Molecular Simulation*, 2013, **39**, 796-821.

18. W. Brown, *Light Scattering: Principles and Development*, Oxford University Press, 1996.

19. P. Matějíček, K. Podhajecká, J. Humpolíčková, F. Uhlík, K. Jelínek, Z. Limpouchová, K. Procházka and M. Spirková, *Macromolecules*, 2004, **37**, 10141-10154.

20. M. Štěpánek, K. Podhajecká, K. Procházka, Y. Teng and S. E. Webber, *Langmuir*, 1999, **15**, 4185-4193.

21. S. Wang, S. Granick and J. Zhao, *Journal of Chemical Physics*, 2008, **129**.

22. E. B. Zhulina and O. V. Borisov, *Macromolecules*, 2012, **45**, 4429-4440.

23. R. Nagarajan and K. Ganesh, *Macromolecules*, 1989, **22**, 4312-4325.